

**Summary**

The sparse, efficient and stable representation of the primary propagator is an important aspect of current prestack depth migration techniques. The primary propagator accounts for one-way wave propagation (downward or upward) from one depth level to the next depth level. It does not account for scattering at boundaries. This paper aims at giving a representation of the primary propagator in the wavelet transform domain and at giving a representation of the seismic data in the wavelet domain. An efficient full prestack migration scheme which uses advantageously the structure of the non-standard wavelet transform, will be derived from these representations. Furthermore, it is shown that the wavelet transform enables the user to choose between resolution and efficiency.

**Introduction**

The Fourier transform reveals the spectrum of a function. Due to the uncertainty relation it is not possible to relate a certain frequency to a certain location of the original function. The wavelet transform is a space-scale analysis tool. It makes it feasible to get an intermediate representation of a function, in which both spectral and spatial information are available. The analysis is done with dilated and translated versions of a basis function  $\psi(x)$ :

$$\psi_{ab}(x) = \frac{1}{\sqrt{a}}\psi\left(\frac{x-b}{a}\right). \quad (1)$$

The translation is covered by the parameter  $b$  and the dilation by the parameter  $a$ . For small values of  $|a|$ , i.e.  $|a| \ll 1$  the wavelet  $\psi_{ab}(x)$  is a highly shrunken version of the function  $\psi(x)$ , which means that it analyzes high frequency aspects around a certain location  $b$ . For large values of  $|a|$ , i.e.  $|a| \gg 1$ , the function  $\psi_{ab}(x)$  is very much spread out, which means that it analyzes low frequency aspects around a location  $b$ . The dilation parameter  $a$  allows to zoom in on local high frequency aspects. In the course of this paper the wavelet transform will be explained further. For an extensive introduction into wavelets the reader is referred to Koornwinder [1993].

Our migration scheme is based upon a data representation derived from the wave equation, which reads for acoustic primary waves in the frequency domain (after decomposition and surface related multiple elimination)

$$\mathbf{P}(\mathbf{x}) = \int W_p^-(\mathbf{x}, \mathbf{x}') \hat{R}^+(\mathbf{x}') W_p^+(\mathbf{x}', \mathbf{x}_S) S_0^+(\mathbf{x}_S) d^3 \mathbf{x}', \quad (2)$$

where  $P^-(\mathbf{x})$  is the flux normalized primary upgoing response of an inhomogeneous half space,  $S_0^+(\mathbf{x}_S)$  is the flux normalized source function for downgoing waves,  $W_p^+(\mathbf{x}', \mathbf{x}_S)$  describes downward propagation of the primary wave from  $\mathbf{x}_S$  to  $\mathbf{x}'$ , the operator  $\hat{R}^+(\mathbf{x}')$  describes reflection at  $\mathbf{x}'$  and, finally,  $W_p^-(\mathbf{x}, \mathbf{x}')$  describes primary upward propagation from  $\mathbf{x}'$  to  $\mathbf{x}$ . Discretization of equation (2) with respect to the horizontal space coordinates leads to the one-way representation for acoustic wavefields introduced by

\*Note that the following position vectors are used:  $\mathbf{x} = (x, y, z)^T$ ,  $\mathbf{x}' = (x', y', z')^T$ ,  $\mathbf{x}_S = (x_S, y_S, z_S)^T$

Berkhout [1982]. This discrete representation will be used to derive an explicit expression for the (angle-dependent) reflectivity matrix  $\mathbf{R}^+$  at all depth levels.

In this paper the spatial wavelet transform is applied to the explicit expression of the reflectivity matrix. It will be shown that the wavelet transform is an efficient tool to weigh up accuracy and efficiency in prestack recursive depth migration.

**Migration in the space domain**

Migration techniques consist of two major steps: firstly, the inverse wavefield extrapolation of the upgoing receiver wavefields and the forward extrapolation of the downgoing source wavefields, correcting for the propagation through the overburden above a certain depth level  $z_m$ . Secondly, the imaging step, relating the source and receiver wavefields at a certain depth level  $z_m$  for all frequencies. These two steps can be made manifest upon rewriting equation (2) in its discretized form (for one depth level), yielding

$$\mathbf{P}^-(z) = \mathbf{W}_p^-(z; z_m) \mathbf{R}^+(z_m) \mathbf{W}_p^+(z_m; z_S) \mathbf{S}^+(z_S), \quad (3)$$

where we have used the kernel representation of the reflection operator  $\hat{R}$ , and where we have assumed a number of general source distributions: each column of  $\mathbf{S}^+(z_S)$  represents one source distribution; each column of  $\mathbf{P}^-(z)$  represents the corresponding receiver wavefield. The result after application of the aforementioned two steps is [Wapenaar and Berkhout, 1989]

$$\mathbf{R}^+(z_m) = [\mathbf{W}_p^-(z; z_m)]^H \frac{\mathbf{P}^-(z)}{S(\omega)} [\mathbf{W}_p^+(z_m; z_S)]^H, \quad (4)$$

describing the full migration process in its basic form. In the derivation the modified matched filter approach has been used as an approximation for the inverse of the primary propagators. Moreover, it is assumed that the source matrix  $\mathbf{S}^+(z_S)$  is a scaled unity matrix (with scaling factor  $S(\omega)$ ). The reader has to notice that equation (4) is an explicit expression for the full angle dependent reflectivity. In a lot of applications the diagonal of  $\mathbf{R}^+$  is used only, which represents the zero-offset reflectivity.

**The wavelet transform**

The continuous wavelet transform is defined by

$$f_{ab} = \int_{-\infty}^{\infty} f(x) \psi_{ab}(x) dx \quad a \neq 0. \quad (5)$$

$f_{ab}(x)$  is the inner product of  $f(x)$  and the (real) function  $\psi_{ab}(x)$  defined in equation (1). Discretization with respect to the parameters  $a, b$  such that  $a = 2^m$  and  $b = 2^m n$  is particularly interesting. Each step in  $m$  corresponds to a bisection of the frequency content. The wavelet transform then elegantly fits into the theory of multiresolution analysis [Mallat, 1989]. The idea of multiresolution analysis is to write a function  $f(x)$  as a limit of successive approximations each of which is a smoothed version of  $f(x)$ , by using more and more concentrated smoothing functions. The successive

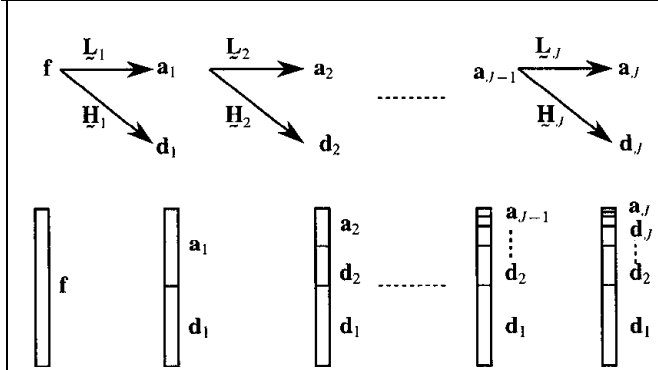


Figure 1: The discrete implementation of the wavelet transform

approximations thus use a different resolution, whence the name multiresolution analysis. The difference between two successive approximations is the detail at a certain resolution. This detail is exactly a wavelet transform for a certain value of  $m$ . The theory of multiresolution analysis and the discovery of orthogonal compactly supported wavelets [Daubechies, 1988] made it possible to implement the wavelet transform as an  $O(N)$ -algorithm. In its discrete implementation the wavelet transform can be interpreted as the successive splitting of an approximation into a detail part and a coarser approximation according to Figure 1.

The approximation matrix  $L_1$ , which operates as a low pass filter, and the detail matrix  $H_1$ , which operates as a band pass filter, divide the original signal (consisting of  $N$  points) in an approximation  $a_1$  and a detail  $d_1$  (both consisting of  $N/2$  points). This step can be repeated upto the coarsest scale, where we are left with the coarsest approximation of the original signal, i.e. with  $a_j$ , and with the coarsest detail, i.e. with  $d_j$  (both consisting of 1 point). Note that the actual wavelet transform consists of a number of details ( $d_1, d_2, \dots, d_j$ ) and the coarsest available approximation ( $a_j$ ). The total amount of samples does not change and an exact reconstruction of the original data is feasible. It is not necessary to apply the wavelet transform all the way down to the coarsest detail  $d_j$  and approximation  $a_j$ , the user can decide at any moment to stop the calculations to end with a certain "coarsest" detail  $d_j$  and a certain "coarsest" approximation  $a_j$  for any  $j = 1, \dots, J$ .

Of special interest is the application of the wavelet transform to 2D-functions. The application to the two axes can be done either independently or dependently. The former case is generally called the standard form, the latter generally the non-standard form [Beylkin et al., 1991]. In Figure 2 the differences between the two forms are illustrated for a general matrix  $M$ . In our application the non-standard form will be used.

#### Migration in the wavelet domain

It has been shown [Dessing and Wapenaar, 1994] that wavefield extrapolation can be carried out in the wavelet transform domain. Coarse approximations of the extrapolation operators already reveal structural information. This knowledge is used in the derivation of a migration scheme in the wavelet transform domain.

The point of departure for the migration in the wavelet transform domain is equation (4). Application of one step of the non-

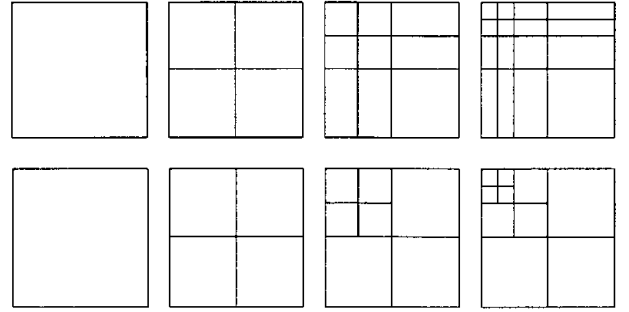


Figure 2: The structure of the standard wavelet transform (top) and the non-standard wavelet transform (bottom) of a matrix. Note that the first step of the standard and non-standard wavelet transform are equal.

standard wavelet transform yields

$$\begin{pmatrix} \mathbf{R}_T^+ & \mathbf{R}_B^+ \\ \mathbf{R}_C^+ & \mathbf{R}_A^+ \end{pmatrix} = \frac{1}{S(\omega)} \begin{pmatrix} \mathbf{W}_T^- & \mathbf{W}_B^- \\ \mathbf{W}_C^- & \mathbf{W}_A^- \end{pmatrix}^H \begin{pmatrix} \mathbf{P}_T^- & \mathbf{P}_B^- \\ \mathbf{P}_C^- & \mathbf{P}_A^- \end{pmatrix} \begin{pmatrix} \mathbf{W}_T^+ & \mathbf{W}_B^+ \\ \mathbf{W}_C^+ & \mathbf{W}_A^+ \end{pmatrix} \quad (6)$$

where the different submatrices for an arbitrary matrix  $M$  of size  $N \times N$  are defined by

$$\begin{pmatrix} M_T & M_B \\ M_C & M_A \end{pmatrix} = \begin{pmatrix} L_1 \\ H_1 \end{pmatrix} M \begin{pmatrix} L_1^T & H_1^T \end{pmatrix}. \quad (7)$$

An efficient scheme results either if the extrapolation matrices in the wavelet transform domain in equation (6) are sparser or if is possible at the expense of some accuracy to neglect parts of the extrapolation operator in the wavelet transform domain. The former is unfortunately not true. The latter is possible (see Figure 3). The neglect of the off-diagonal submatrices  $\mathbf{W}_B^\pm$  and  $\mathbf{W}_C^\pm$  yields

$$\mathbf{R}_T^+ = \frac{1}{S(\omega)} [\mathbf{W}_T^-]^H \mathbf{P}_T^- [\mathbf{W}_T^+]^H \quad (8)$$

$$\mathbf{R}_B^+ = \frac{1}{S(\omega)} [\mathbf{W}_T^-]^H \mathbf{P}_B^- [\mathbf{W}_A^+]^H \quad (9)$$

$$\mathbf{R}_C^+ = \frac{1}{S(\omega)} [\mathbf{W}_A^-]^H \mathbf{P}_C^- [\mathbf{W}_T^+]^H \quad (10)$$

$$\mathbf{R}_A^+ = \frac{1}{S(\omega)} [\mathbf{W}_A^-]^H \mathbf{P}_A^- [\mathbf{W}_A^+]^H. \quad (11)$$

Upon applying the inverse wavelet transform the submatrices  $\mathbf{R}_T^+$ ,  $\mathbf{R}_B^+$ ,  $\mathbf{R}_C^+$  and  $\mathbf{R}_A^+$  can be combined to yield the original reflectivity matrix  $\mathbf{R}^+$ . A simple operation count illustrates the usefulness of the replacement of equation (4) by equations (8)-(11). The amount of computations involved in equation (4) are related to two times  $O(N \times N)$ -matrix multiplications, which correspond to  $2O(N^3)$  operations. The amount of computations involved in equations (8)-(11) is eight times  $O(N/2 \times N/2)$ -matrix multiplications, which correspond to  $O(N^3)$  operations. The latter is half the amount of operations compared with the former. Note that the matrices both in the space domain and in the wavelet transform domain are assumed to be full, which is not completely true. Moreover, the amount of computations related to the wavelet transform are neglected.

The replacement of the computation of  $\mathbf{R}^+$  by the computation of the submatrices of equations (8)-(11) can be repeated for  $\mathbf{R}_T^+$ . The computation of  $\mathbf{R}_T^+$  can be replaced by the computation of four submatrices on again a coarser scale. These steps can be repeated up to the coarsest scale where we are left with four scalar equations. The actual migration in the wavelet transform domain starts at the coarsest scale. By adding the results of the migration at finer scales the resolution can be improved without doing any redundant computations. The amount of work related to the migration in the wavelet transform domain is less than half of the amount of work in the space domain (with the aforementioned restrictions in mind).

### Example

Figure 4 illustrates the quality of the proposed method for a relatively simple macro model (Figure 4a). A full recursive prestack depth migration has been carried out in the space domain according to equation (4) (Figure 4b). A recursive prestack depth migration has been carried out in the wavelet transform domain according to equations (8)-(11) (Figure 4c-f). The combination of these four results (via the inverse wavelet transform) shows the capacity of the proposed method (Figure 4g). For this example the replacement of equation (4) by the more efficient equations (8)-(11) is fully justified.

Moreover, it is observed that the result of the prestack migration according to equation (8) in Figure 4c is almost equivalent with the result of full prestack migration in the space domain (Figure 4). Hence, for this example, only equation (8) can be used to obtain the full prestack migrated result, which corresponds to an efficiency gain of a factor eight (again with the previously mentioned restrictions in mind). The splitting as proposed in the previous section would improve the efficiency even further.

### Conclusions

The non-standard form of the 2D wavelet transform is used to do the migration process in the wavelet transform domain in an efficient way. The wavelet transform enables a stepwise solution of the reflectivity. The process is started with a coarse approximation of the reflectivity. By adding the detail wavefields the resolution of the reflectivity can be improved. The total amount of work in the wavelet transform domain is less than half the amount of work for migration in the space domain.

The stepwise approach gives the user a handle to choose between resolution and efficiency, which feature is directly related to the choice of the non-standard wavelet transform. Depending on the desired resolution the efficiency gain can be large.

### Acknowledgement

The support and the interest of the sponsors of the DELPHI consortium is gratefully acknowledged.

### References

- Berkhout, A. J., 1982, Seismic migration. imaging of acoustic energy by wave field extrapolation: Elsevier.
- Beylkin, G., Coifman, R., and Rokhlin, V., 1991, Fast wavelet transforms and numerical algorithms I: Communications on Pure and Applied Mathematics, 44, 141-183.

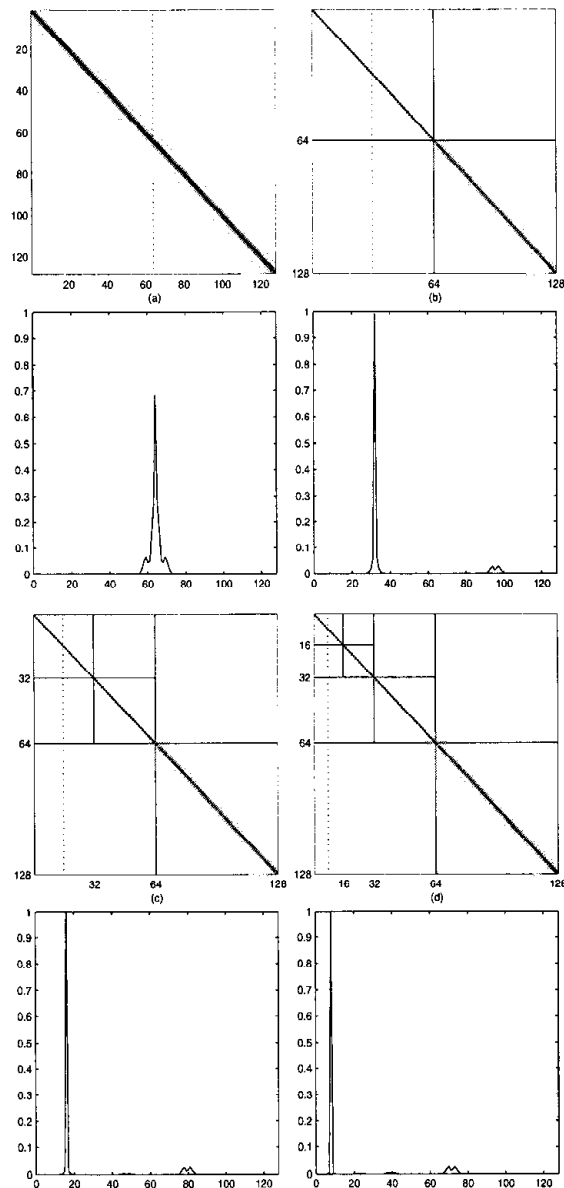


Figure 3: The non-standard wavelet transform for an extrapolation matrix related to a small depth step for a frequency of 30 Hz. The absolute values of the matrix and one column out of the matrix are shown. (a) The space domain extrapolation matrix. (b) One step of the non-standard wavelet transform. (c) Two steps of the non-standard wavelet transform. (d) Three steps of the non-standard wavelet transform. Note that the off-diagonal parts of the transformed matrices can be neglected.

Daubechies, I., 1988, Orthonormal bases of compactly supported wavelets: Communications on Pure and Applied Mathematics, 41, 909-996.

Dessing, F. J., and Wapenaar, C. P. A., 1994, Wavefield extrapolation using the wavelet transform: 64th Ann. Internat. Mtg., Soc. Expl. Geophys., Expanded Abstracts.

Koornwinder, T. H., 1993, Wavelets: An elementary treatment of theory and applications: World Scientific.

Mallat, S. G., 1989, A theory for multiresolution signal decomposition, the wavelet representation: IEEE Transactions PAMI, 11, 674-693.

Wapenaar, C. P. A., and Berkhout, A. J., 1989, Elastic wave field extrapolation: Elsevier Amsterdam.

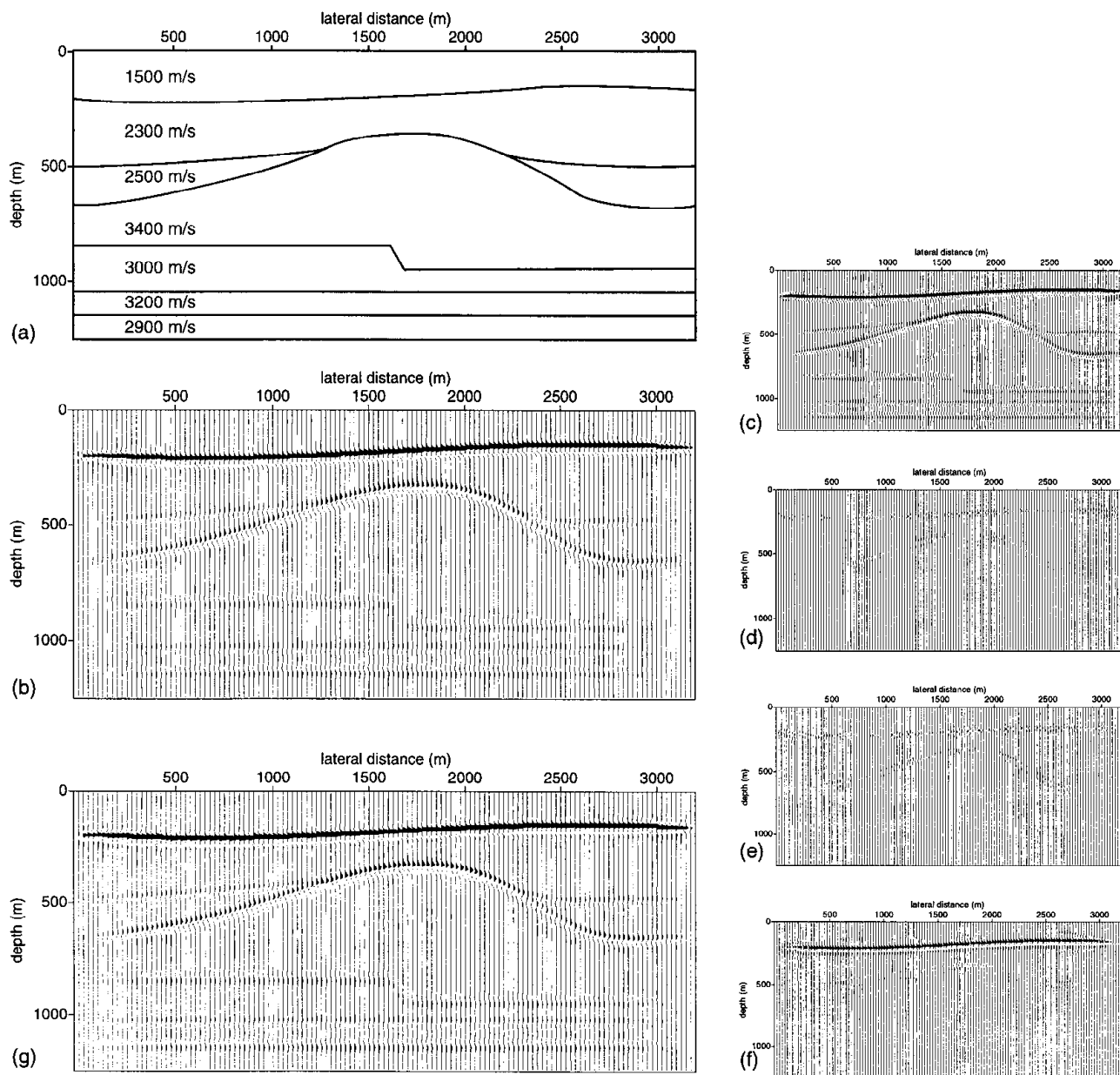


Figure 4: (a) Acoustical model with velocities ranging from 1500 m/s to 3400 m/s. (b) Result of prestack migration in the space domain according to equation (4). (c) Prestack migration according to equation (8). (d) Prestack migration according to equation (9) shown on the same scale as (c). (e) Prestack migration according to equation (10) shown on the same scale as (c). (f) Prestack migration according to equation (11) shown on the same scale as (c). (g) Sum of the prestack migrated results of (c)-(f).

Note that the prestack migrated result of (g) and (b) are almost equal which was to be expected. Moreover, note that the prestack migrated result of (c) obtained with the smooth parts of the extrapolation operators only, already resembles the results of (b) and (g) very well.